SIGNATURES OF TURBULENCE IN THE DENSE INTERSTELLAR MEDIUM

E. FALGARONE[1], T.G. PHILLIPS[2]
[1] *Radioastronomie Millimétrique, Ecole Normale Supérieure, 24 rue Lhomond, 75005 Paris, France*

[2] *California Institute of Technology, 320-47, Pasadena CA 91125, USA*

Abstract. We present an ensemble of recent observational results on molecular clouds which, taken separately, could all be understood by invoking various unrelated physical processes, but taken all together form a coherent ensemble stressing the imprints of turbulence in the physics of the cold interstellar medium. These results are first, the existence of wings in the molecular line profiles, which can be interpreted on statistical grounds as the signature of the intermittency of the velocity field in turbulent flows, second the fractal geometry of the cloud edges, with properties reminiscent of those of various surfaces studied in turbulent laboratory flows, and third, the fact that the dense gas fills only a very small fraction of the space. The last points are supported by CO multitransition observations of a few fields in nearby molecular clouds. They show that the excitation conditions are the same for the gas emitting in the linewings and in the linecores and are also remarkably uniform over a large range (factor 10) of column densities. An attractive interpretation of the molecular line data is that most of the ^{12}CO(J=2–1) and (J=3–2) emissions arise in cold ($T_k \leq 10K$) and dense ($n_{H_2} \sim 10^4\, cm^{-3}$ or more) structures distributed on a fractal set with no characteristic scale size greater than about 1000 AU.

Keywords : Molecular clouds, Turbulence, Intermittency, Linewings, Fractal structure, Self-similarity

1. Introduction

There is considerable evidence from both theory and observations, that gas flows in molecular clouds are turbulent. By this, we mean that in the equations of motion, the non-linear advection term is orders of magnitude larger than the dissipation term. The two Reynolds numbers (hydrodynamic and magnetic, which measure the importance of the non-linear terms in the equations of motion and evolution of the magnetic field respectively) are so large in interstellar clouds that all the characteristics of magnetohydrodynamic turbulence can be expected to be found in their evolution. While the mathematical behavior of the solution of the equation of motion is not yet well understood, the specific manifestations of turbulence in atmospheric and laboratory flows are numerous and it is tempting to view them as diagnostics of turbulence within interstellar clouds (eventhough the effects of magnetic fields and compressibility may be important in the interstellar medium).

Some of these manifestations can be found in the statistics of the velocity field, some others are purely geometrical, all of them are related. In particular, it is now understood that turbulence is highly intermittent, ("the element of surprise in the

E. Falgarone et al. (eds.), Fragmentation of Molecular Clouds and Star Formation, 119–136.

time history of the velocity field", quoting Dutton and Deaven, 1969), especially on the smaller scales, and that many properties, including velocity increments, exhibit distributions that depart significantly from Gaussian in the wings (see references in Falgarone and Phillips 1990). Also, turbulence is not space filling. The subset of the Euclidian space on which the turbulent activity develops is a fractal (Mandelbrot, 1982). Recent high sensitivity measurements in atmospheric and laboratory flows (Anselmet, Hopfinger and Gagne, 1984; Méneveau 1989) allow a quantitative approach to the fractal structure of the subset of space on which the dissipation of turbulence is concentrated and connect it to the intermittency of the velocity field.

These observable signatures of turbulence are present in molecular clouds. In this paper, we discuss first the information relevant to the velocity field contained in the molecular lineshapes and second that contained in the spatial and density structure of molecular clouds.

2. Molecular lineshapes

2. 1. INTERSTELLAR LINEWINGS

It has been clear for a long time that the linewidths of molecular transitions, as seen in emission from regions of the dense interstellar medium, are too large to be simply due to the thermal motions of the molecules. Typical linewidths from molecular clouds are in the 0.5 to 2 $km\,s^{-1}$ range for the relatively quiescent regions and of course can be much greater for disturbed regions. However, the thermal width for the CO molecule is only about 0.05 $km\,s^{-1}$ for a typical kinetic temperature of 10−20 K. Zuckerman and Evans (1974) suggested that this might be due to the effect of turbulence, but the characteristic signature of turbulence was not fully understood at that time. A major step forward was made by Larson (1981) who showed that the linewidths scale with the size of the region under study, roughly as predicted by Kolmogorov for the case of incompressible turbulence. This is suggestive of a turbulent origin to the linewidths, but there could be many other effects which would give a comparable scaling of the linewidth with size, including statistical effects (see the review of Scalo, 1987). An additional characteristic of the kinematics of molecular clouds is the existence of broad wings in the molecular line profiles often observed in the direction of clouds not associated with molecular outflows. The wing emission has been shown to be optically thick (Magnani, Blitz and Wendel 1988) and has received several interpretations. Keto and Lattanzio (1989) proposed that it could be generated by cloud collisions, Magnani et al. (1990) claimed that it arises in gas less dense than $10^3\,cm^{-3}$, and Elmegreen (1991) invokes magnetosonic waves in molecular clouds with the broad wings originating in regions of low average density where the Alfvén velocity increases.

Our approach to this problem has been to study, in a statistical way, the full profiles of the molecular lines to extend the information beyond the behavior of just the linewidths and propose an interpretation which is scale-independent (Falgarone and Phillips, 1990).

https://doi.org/10.1017/S0074180900198845 Published online by Cambridge University Press

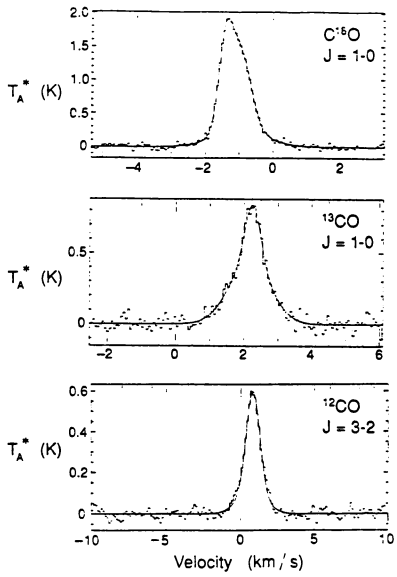

Fig. 1. Spectra of CO emission for various isotopes and ladder lines in non-starforming regions of *(a)* Auriga, (Falgarone, Puget and Pérault 1991), *(b)* Ursa Major (Falgarone and Pérault 1988), and *(c)* Taurus-Perseus (Falgarone, Phillips and Walker 1991). The lines have excess strength in the wings as compared to a Gaussian profile, but very high signal to noise ratios are needed to discriminate the wide wing structure in these relatively weak lines. The continuous lines are least square fits of a narrow Gaussian (two for the $C^{18}O$ spectrum) plus a weaker broad Gaussian.

The essential point is that turbulence studies show that the velocity distributions are non-Gaussian to some degree. There is a fundamental property of turbulence called intermittency which predicts that there is an excess of large velocity deviations in a given region as compared with a Gaussian distribution of velocities. For the interstellar medium this means that, if we consider the line profiles as the tracers of the probability distribution of the velocity differences, the linewings are enhanced. Some examples of non-Gaussian spectra in typical non-starforming regions are shown in Figure 1. In this conference paper and in Falgarone and Phillips (1990) we attempt to describe the nature of intermittency and to relate molecular lineshapes to the predictions of turbulence models.

2. 2. THE TURBULENT CASCADE

In 1941, Kolmogorov predicted the self-similar behavior of the velocity field in incompressible turbulent flows by postulating the existence of a local dissipationless cascade of kinetic energy from large scales to small scales in which large 'eddies' become unstable and split into smaller and smaller 'eddies'. L_0 is the large scale size at which the energy is injected into the cascade and λ_0, the small scale size at which the kinetic energy is dissipated and is transferred to another process such as heating of the fluid. He predicted that at scales $\lambda_0 << \ell << L_0$, the distribution of the velocity field is determined only by the mean dissipation rate of specific kinetic energy $\bar{\epsilon}_d$. Dimensional arguments give the scaling with ℓ of the n^{th}-order moments of the increments of the velocity field

$$M_n = <| \mathbf{v}(\mathbf{r}+\ell) - \mathbf{v}(\mathbf{r}) |^n> \propto (\bar{\epsilon}_d \ell)^{n/3} \qquad (1)$$

This relation is statistical, not deterministic, and the brackets hold for an ensemble average.

https://doi.org/10.1017/S0074180900198845 Published online by Cambridge University Press

However, any model for turbulence, or whatever the semantic description of the highly non-linear process may be, must be subject to experimental test. Kolmogorov's prediction was later modified (Landau and Lifchitz 1959; Kolmogorov 1962; Oboukhov, 1962) when laboratory experiments showed that the dissipation rate of specific kinetic energy, ϵ_d, was not uniform, but concentrated in an intermittent fashion into the limited regions of space and time where velocity gradients reach large values or diverge.

Much work has been done in this area in laboratory duct flows and in the Earth's atmosphere. In particular Dutton and Deaven (1969) carried out well defined measurements of the velocities in turbulent flows where they could monitor the velocity differences, as a function of time, between two points separated by a variable distance r along the flow. They discovered an excess of large velocity differences as compared to a Gaussian distribution, which they ascribe to the intermittency of turbulence. Figure 2 shows more modern measurements by Van Atta and Park (1971) of the probability density of the velocity differences in the atmosphere above the Ocean, clearly indicating the excess of large velocity dispersion events.

2. 3. INTERMITTENCY

In order to take into account the clearly modified scaling due to the intermittency of ϵ_d, Kolmogorov introduced a modified scaling law for the moments

$$M_n \sim \bar{\epsilon}_d{}^{n/3} \ell^{\zeta_n},$$

where ζ_n was permitted to deviate from $n/3$. Several theoretical approaches predict simple analytical forms of ζ_n. For a log-normal distribution of the energy dissipation rate averaged over a volume of size ℓ (Kolmogorov, 1962), $\zeta_n = \frac{n}{3} - \frac{\mu}{18} n(n-3)$. Alternatively, for the β-model of Frisch et al. (1978) in which the eddies are less and less space filling as their size decreases, $\zeta_n = \frac{n}{3} - \frac{1}{3}\mu(n-3)$.

The constant μ is called the intermittency parameter. Neither model is correct although they are quite a good approximation for most of the low order moments ($n \leq 6$). More recent models of greater complexity (e.g. the multifractal formalism, Méneveau 1989) differ again in the algebraic form, but the concept of a small n-dependent modification to the scaling, whose magnitude is a measure of the intermittency, is still retained.

It is particularly important to note that the high order moments contain the information on the intermittency and that intermittency exists at all scales, being relatively more pronounced, as the sizes decrease.

2. 4. RELATION OF INTERSTELLAR SPECTRA TO THE MOMENT ANALYSIS AND ATMOSPHERIC FLOWS

The observation of an interstellar line involves the integration of emission from a cylindrical volume of diameter d and length D, representing the telescope beam

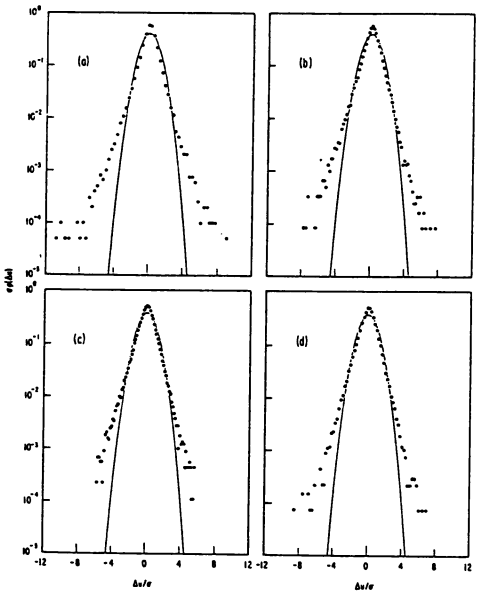

Fig. 2. Probability densities of the velocity difference for various values of the separation r : (a) r=1.38cm, (b) r=4.14cm, (c) r=9.67cm, (d) r=20.7cm. The distribution is clearly in excess of Gaussian (full curves) for large values of the relative velocity difference. The logarithmic scale for the probability distribution emphasizes the behavior at large velocity separations (from van Atta and Park 1971).

through the molecular cloud. We expect to see through the cloud, because the velocity gradient is high in regions of intermittency. The average separation of points within the tube is :

$$\bar{\ell} = \frac{D}{2\sqrt{3}} \left(1 + \frac{2d^2}{D^2}\right)^{1/2}$$

Returning to the moment description we can write :

$$M_n = \int p(\delta v)\ \delta v^n\ d(\delta v),$$

where the probability density is given in terms of the emission strength, T_A^*, by

$$p(\delta v) = T_A^*(\delta v) \Big/ \int_{\text{line}} T_A^*\ dv.$$

In principle this allows the computation of the moments and a test of the scaling laws. We make the simplifying assumption that any line profile is associated with

https://doi.org/10.1017/S0074180900198845 Published online by Cambridge University Press

the separation $\bar{\ell}$. However, the data set must fulfill a number of conditions, such as *(i)* a very large range in the probability density, or extremely high signal to noise ratios, particularly in the far line wings, *(ii)* a very large range in spatial separations ($\bar{\ell}$), i.e. in beam and cloud sizes, *(iii)* if possible (and at least for nearby clouds) it must avoid star-forming regions, to eliminate extra zones of injection of energy into the cascade.

An ideal data set would be a fully sampled, very large map of a nearby non-starforming cloud, with very high signal to noise in each pixel. Variation in $\bar{\ell}$ would be obtained by averaging areas of the cloud ranging from one pixel to the whole cloud. Since this is beyond the capabilities of current instrumentation, we have used a set of 20 molecular line spectra, built on data from the literature, ongoing work (Falgarone, Puget and Pérault 1991), unpublished spectra from M. Pérault and H. Ungerechts, and our own measurements. It involves an ensemble of clouds of various sizes at various distances, which gives a range for d from less than $0.1\,pc$ to more than $100\,pc$, or more than 3 orders of magnitude. The data is summarized in Table 1 of Falgarone and Phillips (1990).

2. 5. ANALYSIS OF THE DATA

In an ideal data set it would be possible to analyze each spectrum for the various moments. In fact, for reasons of finite signal to noise, we have to characterize the profiles with an analytic form in order to make progress. We have chosen to use a two Gaussian fit (core and wing Gaussians of velocity dispersions σ_c and σ_w respectively) as shown in Figure 3. This is physically reasonable and also has the necessary property that high order moments converge. A Gaussian core and exponential wing is another possibility. It is a slightly worse fit, but if adopted, does not change the conclusions. The result of the fitting procedure is that we observe a constant scaling with $\bar{\ell}$ such that

$$\frac{\sigma_w}{\sigma_c} = 3.3\,(\pm 0.2)$$

over the full range of $\bar{\ell}$. In other words, the existence of wings is an intrinsic property of the clouds over scale sizes less than $0.1\,pc$ to more than $100\ pc$ and the wings and cores scale similarly with the size. The entire line profile is therefore self-similar.

The moments can be obtained from the two Gaussian fits. The first moment, M_1, is related to the linewidth and we find that the slope, ζ_1, is close to the value 0.33 required by the Kolmogorov scaling. Care is needed in deducing the slope of the data shown in Figure 4 because of the need to know the errors on both axes. For our best estimate of the shapes of the error boxes we find $\zeta_1 = 0.33$, but with a possible range extending from .28 to 0.37.

Information on the intermittency parameter is contained in the higher order moments. If we can rely on the assumption that the Gaussian (or exponential) fits to the wings are valid to $\Delta v = \infty$ then the higher moments are given by :

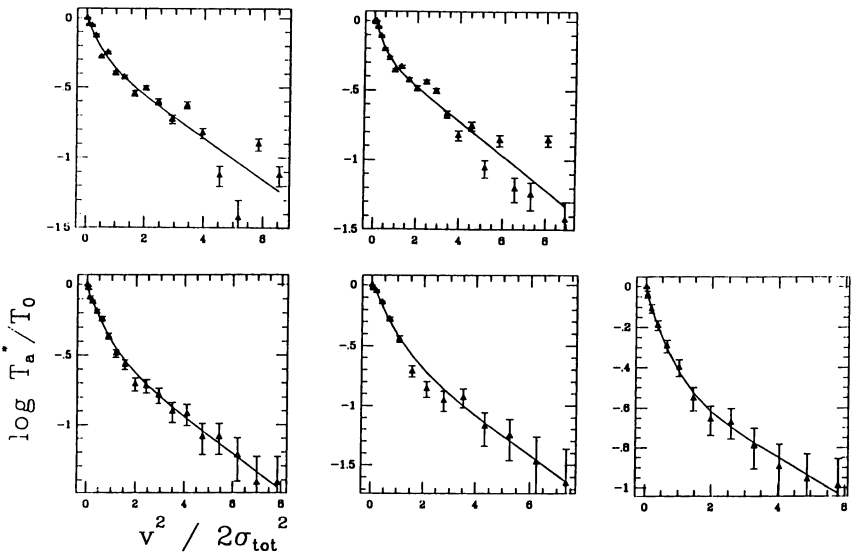

Fig. 3. Linear-log display of the five (out of six) half-profiles of Figure 1 which present linewing excess emission. They have been normalized to the peak temperature and $\pm 1\sigma$ error bars are shown. The choice of coordinates is such that Gaussians appear as straight lines.

$$M_n \propto \frac{a_w \sigma_w^{n+1}}{\int_{\text{line}} T_A^*(v)\, dv}$$

where a_w is the amplitude of the wing Gaussian, and

$$\zeta_n = \frac{d \ln(M_n)}{d \ln(\bar{\ell})}.$$

We can plot the $\bar{\ell}$ dependence of a_w, σ_w and the line integral to deduce μ. If we compare with the model of Frisch et al. (1978) we get $\mu \sim 0.1$. The values found for atmospheric measurements are ~ 0.2 (Anselmet, Gagne and Hopfinger, 1984). However, the accuracy in the interstellar measurements is currently very poor and much higher signal to noise spectra are needed.

https://doi.org/10.1017/S0074180900198845 Published online by Cambridge University Press

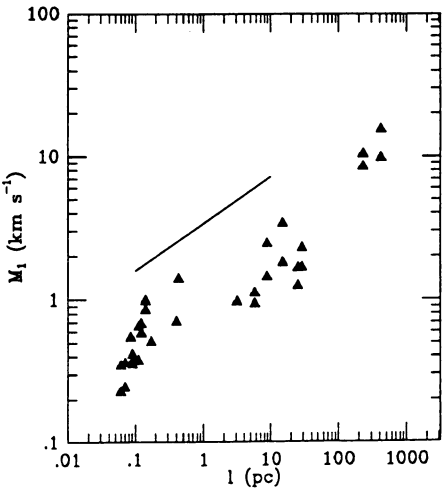

Fig. 4. Dependence of the first order moment of the line profiles on the characteristic dimension $\overline{\ell}$ adopted for each emitting region. The slope 1/3, predicted by Kolmogorov for incompressible turbulence, is shown for comparison.

3. The spatial structure of molecular clouds

3. 1. THE SELECTION OF THE OBSERVED FIELDS

The second part of the argument relies on a different data set consisting of an ensemble of maps of inactive parts of molecular complexes, taken at high angular resolution with the 10m antenna of the Caltech Submillimeter Observatory (CSO) in the ^{12}CO and ^{13}CO (J=2–1) and (J=3–2) transitions (Falgarone, Phillips and Walker 1991). The fields selected for observations are almost transparent when viewed at low angular resolution. *At the parsec scale*, they have a low average H_2 column density $N_{H_2} \leq 10^{21}\, cm^{-2}$. The low *average* column density of matter ensures little crowding of emitting elements along the line of sight. This spatial transparency in principle allows a better view of the structure, its degree of convolutedness and its shape, because details do not blend with each other. In addition, the fields have been selected to include velocity components which belong both to the center and to the extreme wings of the velocity distribution of the entire complexes. It is this specific point which allows an elucidation of the connection between the velocity field at all scales within a complex and the density structure at very small scale, in the broad context of turbulence. The overall velocity distribution in a complex can be obtained with very good signal to noise ratio by summing all the individual spectra of a well-sampled map of this complex. The grand average spectra of the Taurus-Perseus-Auriga and Cygnus OB7 complexes, which would be those obtained with large beamsizes of $\sim 100\, pc$ and integration times of several hundreds hours, are shown in Figure 5. They were provided by H. Ungerechts and M. Pérault respectively, who integrated all the spectra of the

large scale maps (Ungerechts and Thaddeus, 1987; Falgarone and Pérault, 1987). The velocity offsets of the gas components studied individually at high angular resolution are shown on these grand average spectra. Our targets therefore include gas representative of material emitting in the low brightness wings of complexes as well as in the line cores.

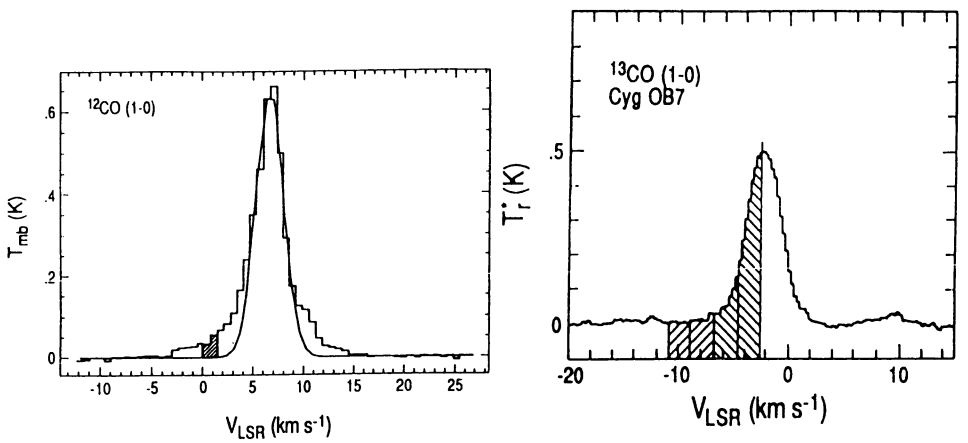

Fig. 5. The grand average spectra. *(a)* ^{12}CO(J=1–0) integrated profile of the Taurus complex. The 3817 individual spectra of the $\sim$ 750 square degrees map have been added (H. Ungerechts, private communication). *(b)* ^{13}CO(J=1–0) integrated profile of the CygOB7 complex. About 3000 individual spectra of the $\sim$ 20 square degree map have been added (M. Pérault, private communication). The velocity coverage of the gas components studied individually at high angular resolution are hatched intervals.

It is nevertheless possible that the structure we see across the edges of molecular clouds is not representative of that of the bulk of the molecular material. In regions where UV photons are pervasive, the chemistry could be different and the CO abundances may not have reached the value they have in more shielded regions. There could be large fluctuations of molecular abundances from one position to another which would mimic variations of the total gas column density. Probably, this is not the case. In recent studies of molecular clouds, starting with the CI studies (Phillips and Huggins,1981; Keene et al., 1985; Genzel et al. 1988; Zmuidzinas et al., 1988) and reinforced by CII work (Stutzki et al. 1988; Boreiko, Betz and Zmuidzinas 1990), it has become clear that the interior regions of molecular clouds are more similar to the edge regions than might be expected. In particular, the similarity of the entire line profiles in the ^{13}CO and CI lines observed by Frerking et al.(1989) in ρ Ophiuchus strongly suggests that shielded

https://doi.org/10.1017/S0074180900198845 Published online by Cambridge University Press

and unshielded material in molecular clouds are intimately mixed with each other not only in space, but also in velocity space. This is also shown by the tendency for molecular species to be observed in interior regions where it might have been expected that they should be condensed on dust grains. In other words, from a chemical point of view, there is much in common between the interiors and the edges of clouds. A probable explanation is that the UV penetrates much deeper into the clouds than anticipated, due to what is usually described as 'clumpy structure' (Boissé, 1990). Thus, we feel confident in using the edges of the clouds in velocity and space as useful regions to probe the cloud material because of their transparency. The target selected in the Taurus complex is shown in Figure 6.

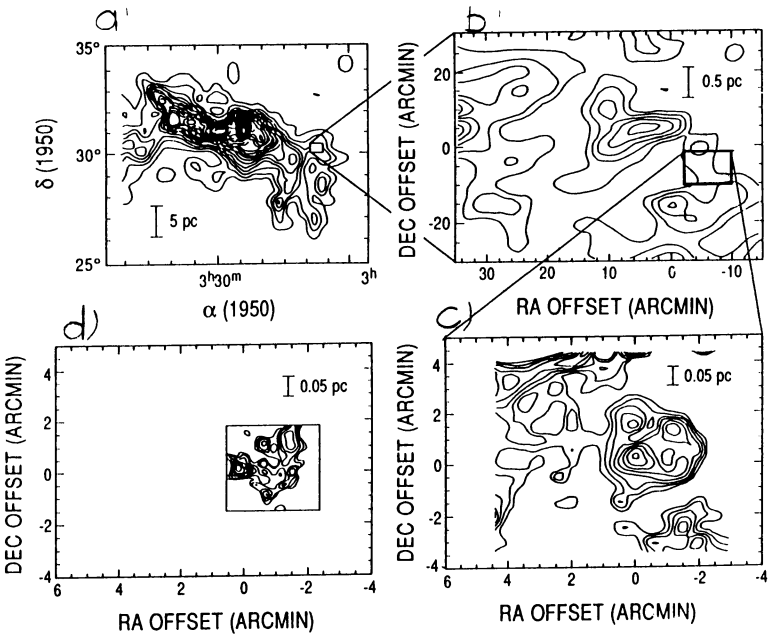

Fig. 6. *(a)* The field studied at high angular resolution, located on the appropriate fragment of the Ungerechts and Thaddeus velocity-integrated intensity map. First contour $0.5\,K\ km\ s^{-1}$, step $1.5\,K\ km\ s^{-1}$. *(b)* Velocity-integrated intensity of the ^{12}CO (J=2–1) emission (CSO, HPBW=30", sampling 5'). First contour $2\,K\ km\ s^{-1}$, step $2\,K\ km\ s^{-1}$. Reference position $\alpha(1950) = 3h\ 07m\ 27.4s$, $\delta(1950) = 30°\ 05'$. *(c)* Velocity-integrated intensity of the ^{12}CO (J=2–1) emission (CSO, HPBW=30", sampling 30") within the area delineated in *(b)*. First contour $1.8\,K\ km\ s^{-1}$, step $0.3\,K\ km\ s^{-1}$. Reference position $\alpha(1950) = 3h\ 06m\ 54.9s$, $\delta(1950) = 29°\ 58'$. *(d)* Velocity-integrated intensity of the ^{12}CO (J=3–2) emission (CSO, HPBW=21", sampling 18"). First contour $0.85\,K\ km\ s^{-1}$, step $0.2\,K\ km\ s^{-1}$. Same reference position as in the previous map. The linear scales are computed for a distance to the cloud $d = 200\,pc$.

https://doi.org/10.1017/S0074180900198845 Published online by Cambridge University Press

3. 2. RESULTS OF THE CO MULTITRANSITION OBSERVATIONS

All the data, in particular those from the remote fields at 750pc, are presented in Falgarone, Phillips and Walker (1991). The raw observational results are the following. First, for all the fields, and both transitions, spatial structure exists at all size scales down to the best angular resolution, which, in the case of the Taurus field and the high frequency beam, is $0.02\,pc$ or 4000AU (see Figure 6d).

Second, for all the fields, the maximum peak line intensities in the maps are comparable and low, $T_A^* \sim 3$ to $5K$ in both CO rotational lines, in spite of an anticipated variation of the beam dilution between the remote and nearby fields of $\left(\frac{750}{200}\right)^2 = 14$. In the simple picture of a clumpy medium, this result combined with the first one would imply that the emission arises in fragments much smaller than the smallest beam.

Third, the integrated intensity maps are remarkably self-similar. The maximum brightness contrast observed in a map scales with the size over which it is observed, and Taurus and Cygnus, although at very different distances from the Sun, exhibit the same brightness contrast over comparable distances.

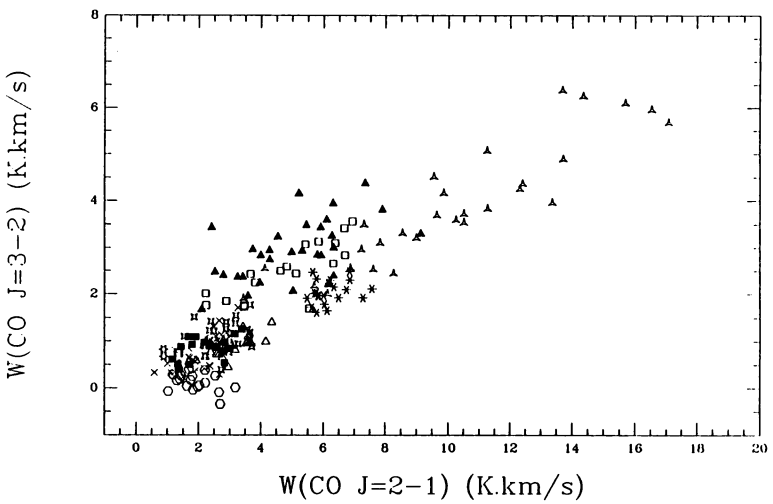

Fig. 7. ^{12}CO (J=3–2) versus ^{12}CO (J=2–1) integrated intensities (uncorrected for beam efficiency) for all the fields and velocity components. Solid symbols are for two core velocity components in CygOB7. Empty squares and triangles (starred or not) are for the four wing velocity components of these two fields. The data from the Taurus fields are the crosses and the asterisks. Empty hexagons indicate upper limits for the ^{12}CO (J=3–2) line. Note the absence of any trend for the solid symbols (linecore velocities) to be distinguished from the empty ones (linewings velocities). There is also no distinction between the remote (Cygnus OB7) and nearby (Taurus) fields.

https://doi.org/10.1017/S0074180900198845 Published online by Cambridge University Press

Fourth, the (J=2–1) and (J=3–2) integrated intensities stay approximately proportional to each other over the entire range of values accessible to our observations (Figure 7). In particular there is no tendency for their ratio $R = \frac{W(3-2)}{W(2-1)}$ to increase as the ^{12}CO(J=2–1) integrated intensity, $W(2-1)$, increases by a factor as large as $\sim$ 10, nor to vary with either the velocity range or the size of the emitting region. There is some significant scatter of the values of R from field to field, and component to component and even within components, but there is no indication of systematic variation with either the column density or the velocity. The ensemble of data is consistent with $R = 0.55 \pm 0.2$. Uncertainties affect the above average value R = 0.55 and are extensively discussed in Falgarone, Phillips and Walker (1991).

A fifth result is that the gas is optically thick in ^{12}CO (J=2–1). Our estimate, $2.5 < \tau_{CO(2-1)} < 6.5$, relies on the assumption of a similar excitation temperature for both isotopes, and an isotopic abundance ratio $[^{12}CO]/[^{13}CO] = 57$, (Langer and Penzias, 1990). Even for the lowest possible abundance ratio, the ^{12}CO (J=2–1) optical depth would remain larger than one.

Some immediate conclusions can be drawn from the raw observational results :
(i) the self-similarity of the maps, with structure at all scales down to the resolution size, suggests a fractal geometry for the CO emitting gas.
(ii) the uniformity of the ratio R (Figure 7) means that the observed gas has comparable excitation properties in all the fields, independent of their size and their velocity with respect to the centroid velocity of the complex.

3. 3. THE SPATIAL SELF-SIMILARITY

The self-similarity of the CO maps in non-starforming regions can be illustrated by the fact that it is impossible in general by simple inspection of a map of antenna temperature for which the contour levels are known, to guess its linear extent. It is possible to quantify this self-similarity by estimating the fractal dimension of the CO contours by the method of the area-perimeter relation which uses the property that for a curve of fractal dimension D_2 in a plane, the perimeter and area are related by $P \propto A^{D_2/2}$. Lovejoy (1982) applies this method to atmospheric clouds and rain areas of sizes ranging between 1km and 10^4km and measures a fractal dimension $D_2 = 1.35 \pm 0.05$. In the Taurus complex, Falgarone, Phillips and Walker (1991) have found the same dimension, $D_2 = 1.36$, for the large scale ($\sim 25°$) ^{12}CO(J=1–0) map of Ungerechts and Thaddeus (1987), for the $\sim 1°$ undersampled map in the ^{12}CO(J=2–1) line and for the $\sim 8'$ maps in the ^{12}CO(J=2–1) and (J=3–2) lines (Figure 8). It is remarkable that this dimension is the same for maps in three different rotational transitions of CO which in principle are sensitive to gas of different densities. It is also comparable to that found for other column density tracers of the cold interstellar medium, the IRAS 100μm emission in the Taurus complex (Scalo, 1990), in a high latitude cloud (Bazell and Désert, 1988) and for the HI emission in a high velocity cloud (Wakker 1990). The fact that whichever tracer is used, the fractal dimension is roughly the same suggests that lower density

molecular gas and even atomic gas are distributed on a set which has the same fractal topology as denser gas, for instance that seen in ^{12}CO(J=3–2). This value is indicative of a possible link between the topology of the cold interstellar medium and the role of turbulence in structuring it.

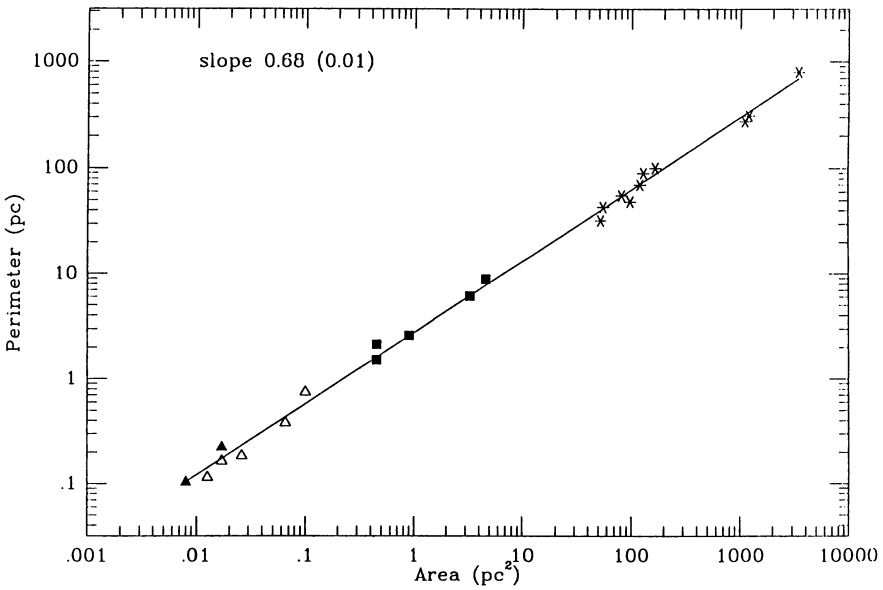

Fig. 8. Perimeter versus area of contours of integrated emission in the large scale ^{12}CO (J=1–0) map of Ungerechts and Thaddeus (1987) (asterisks), the undersampled ^{12}CO (J=2–1) map (empty squares) and the well sampled ^{12}CO (J=2–1) (empty triangles) and (J=3–2) (solid triangles) maps. The perimeters have all been scaled to the resolution $\epsilon = 30'$ of the (J=1–0) map, according to $P(\epsilon) \propto \epsilon^{1-D_2}$. The slope of the perimeter-area relation is $D_2/2 = 0.68$.

Sreenivasan and Méneveau (1986) measure the fractal dimension (D_2') of the curves obtained by 2-dimensional slicing of a variety of interfaces in turbulent flows. Their remarkable result is that, for several interfaces and surfaces (of isoconcentration or isodissipation of the kinetic energy), they find the same dimension, $D_2' = 1.36$. D_2' may differ from the dimension D_2 of the projection onto a plane of a fractal surface of dimension D_3, but limited experiments suggest that $D_2' \leq D_2$ (see Méneveau 1989). If isotropy is assumed, one can write $D_3 = D_2 + 1$. The same authors show that a dimension $D_3 = 7/3$ (in Euclidian space) can be predicted for any kind of interface in a turbulent flow in which the velocity scaling law can be written $\delta v \propto \delta \ell^{1/3}$.

Although it is not clear yet what conclusions could be drawn from the similarity of the dimensions among these various systems or what is due to mere coincidence,

https://doi.org/10.1017/S0074180900198845 Published online by Cambridge University Press

a remarkable consequence of the fractal geometry is that the quantities which describe the spatial distribution of matter are determined by expressions which differ notably from those of an ensemble of randomly distributed clumps. The number $\mathcal{N}(l)$ of structures of linear dimension l in a fractal of dimension D_3 scales as :

$$\mathcal{N}(l) = \left(\frac{L_0}{l}\right)^{D_3}$$

where L_0 is a normalization parameter determined by the observed number of structures of a given size in a map. From the maps in the Taurus field (Figure 6), we find $L_0 \sim 50\,pc$ by estimating that ~ 10 structures of $\sim 10'$ are present in the map. The volume filling factor of the ensemble of structures of size l is therefore

$$f_v(l) = \left(\frac{L_0}{l}\right)^{D_3-3} \tag{2}$$

and their surface filling factor

$$\eta_s(l) = \frac{L_0^{D_3-3}}{l^{D_3-2}} \times s \tag{3}$$

where s is the length along the line of sight of the volume occupied by the entire structure.

The paradoxical consequence of the fact that $2 < D_3 < 3$ is that the area filling factor increases as the structure size decreases while the volume filling factor keeps decreasing with l. For $D_3 = 2.36$, $\eta_s(l) \propto l^{-0.36}$ and $f_v(l) \propto l^{0.64}$. This implies that any beam is predominantly filled by the smallest structures. Another characteristic of such a structure is that the mass within any volume of projected size L scales as L^2, which seems to be the scaling law found for molecular clouds over a large range of sizes.

3. 4. THE PHYSICAL PARAMETERS OF THE GAS

Since the ratio R of the J=3-2 and J=2-1 transitions is a very sensitive measure of the relative excitation temperatures of the two transitions, the lack of systematic variation of this ratio with the column density and the relatively small amount of scatter (Figure 7), might indicate that a universal density, velocity and temperature structure, on size scales much smaller than the beam, conspires to give a uniform ratio. At present, we are not able to evaluate this situation in a computational way because it would require an analysis which includes the density-velocity correlation as developed by turbulence.

Fortunately, in trying to deduce the physical parameters of the gas distribution, it is possible to use the general properties of self-similarity of the molecular cloud structure as exemplified by the fractal nature of the cloud edges and the similarity of the maps in the Taurus and Cygnus fields. We do not attempt to derive a density

structure from the observations but favor solutions in which all the ^{12}CO(J=3–2) and (most of) (J=2–1) emission arises in cold and dense structures distributed on a fractal set. This solution, in which the excitation conditions are uniformly close to thermalization is preferred for the following reasons :

(i) quasi-thermalized cold gas naturally explains the low peak antenna temperatures without invoking beam dilution, or excitation temperatures, which would be systematically lower in nearer sources in order to reproduce the similarity of the observed peak values in fields at different distances. Low values of R imply $T_k \leq 10K$, since in this case R only depends on the kinetic temperature. Furthermore, it allows for values of the beam filling factor $\eta_s > 1$.

(ii) dense gas is needed to build up the CO column density required to reproduce the observed line integrated intensities in the smallest structures (Figure 6), without invoking unrealistically large CO abundances.

In this picture, small scale brightness fluctuations in the maps are due to variations of the crowding of structures much smaller than the beam size from one line of sight to the next. Variations of the line ratio R most likely trace those of the kinetic temperature. Also, we can use the dependence of η_s with l given in (3) to derive the maximum size l_{max} for which $\eta_s = 1$. It is :

$$l_{max} = 1000AU \left(\frac{L_0}{50\,pc}\right)^{-1.8} \left(\frac{s_{max}}{2\,pc}\right)^{2.78} .$$

It is interesting to note that the volume filling factor of the ensemble of these structures in a molecular complex of size $L_0 = 50\,pc$ is $f_v = 2\ 10^{-3}$, which is remarkably small.

Our results on the uniformity of excitation conditions of dense gas in non-starforming regions are in harmony with recent observations which also suggest a remarkable homogeneity of the excitation conditions in quiescent molecular clouds and may support the idea that the cold interstellar medium is made of tiny dense structures. Values of the CS(J=2–1)/CO(J=1–0) ratio observed in the Galaxy far from star forming regions and in external galaxies are shown in Figure 2 of Falgarone (1991). It is a compilation of data from Drdla et al. (1989), Mooney and Solomon (1990), Sage et al. (1989) and Mauesberger et al. (1989). There is no trend for this ratio, usually considered as a tracer of dense gas, to increase toward small scales. There is an important scatter in the ratios, but no trend of systematic variation with for example the CO integrated brightness Casoli et al. (1991) show that the ratio of the CO(J=2–1) to (J=1–0) emissions in the disks of a large variety of galaxies is low (between 0.5 and 0.8) and remarkably uniform and does not depend on the size of the emitting region between 50 pc and 25 kpc. These results are unlikely to be biased by optical depth effects since Falgarone, Puget and Pérault (1991) find also uniform and low values 4of the same ratio for the ^{13}CO lines in the direction of quiescent clouds.

The idea that the bulk of the CO emission of molecular clouds arises in cold thermalized gas is not new. In 1972, Penzias et al. derived from their CO observations of dark clouds that the J=1-0 emission is thermalized and that most clouds

have kinetic temperature near 6K. More recently, Clemens and Barvainis (1988) find a sharp maximum at $T_R \sim 4K$ in the histogram of the ^{12}CO(J=2–1) peak temperatures of 248 small molecular clouds and conclude that most of the cataloged clouds are cool with kinetic temperatures $\sim 8K$. What is new is that the same results are now found over a very large range of sizes, with a spectacular self-similarity, a fact which cannot be easily dealt with in a simple clumpy structure. The fractal geometry, in turn, may allow us to understand why the previously believed isolated clouds are in fact connected by widespread emission at a very low level, as revealed by recent CO observations of large areas of the sky, down to unprecedented sensitivity limits (Heithausen and Thaddeus, 1990; Lee, Snell and Dickman, 1990).

4. Conclusions

We have interpreted several characteristics of the molecular line emission of the cold interstellar medium as a manifestation of the importance of turbulence in structuring the velocity field and the spatial distribution of dense gas, from the smallest to the largest sizescales.

Our analysis of the shapes of the molecular line profiles relies on an ensemble of 20 spectra of high signal to noise ratio, from emitting regions whose sizes range from less than 0.1pc to more than 100pc. We reach the following conclusions :

1. For all accessible scale sizes, a significant fraction of the mass of molecular clouds has unexpectedly high velocities relative to the cloud centroid velocity and provides the origin of the broad spectral wings. Considering the line profiles as tracers of the velocity probability distribution of the gas along the line of sight, we propose that the wings represent a direct observational signature of the intermittency of the velocity field, an intrinsic property of turbulence observed in atmospheric and duct flows.

2. Most of the line profiles can be described with a core and a wing Gaussian whose widths are both found to scale self-similarly with size. Kolmogorov scaling apparently applies to the entire profiles, with an exponent near 1/3, which is that predicted for incompressible turbulence. Our interpretation of the linewings implies the self-similarity of the entire lineshape with size.

3. It is hard to measure the value of the intermittency parameter and we find a smaller value ($\mu \sim 0.1$) than in atmospheric studies ($\mu \sim 0.2$). Line profiles extending to 20 times the half width are ideally required to accurately determine μ.

We then show that the spatial structure of clouds is amenable to observations if regions are chosen near the edges of both the spatial and velocity distribution of complexes, so that the information is not obscured by crowding of structures along the line of sight. Fields in Taurus and Cygnus OB7 were chosen with this criterion in mind. Our conclusions regarding the spatial distribution of gas are :

4. CO maps at various scale sizes and resolutions exhibit self-similarity. The fractal dimension D_2 is measured by means of the area-perimeter relation and is

about 1.36 in the Taurus complex, in large and small scale maps and whichever rotational transition of CO is used. This fractal dimension is comparable with that found earlier in HI maps of high velocity clouds, and $100\mu m$ maps of the dust emission of nearby clouds.

5. The ratio R of CO(3-2) to CO(2-1) intensities is relatively constant in all the fields, $R \sim 0.5$. It somewhat fluctuates from field to field or component to component but does not show any systematic variation with either the total column density of gas (over a factor of 10), or the size of the region, or its velocity relative to the bulk of the gas. The excitation conditions of the gas in non-starforming regions are therefore quite uniform over a large range of conditions.

6. The concept of fractal structure helps us to understand the density structure of molecular clouds. Together with a measure of the optical depth estimated from ^{13}CO measurements, we use it to show that the CO(J=2–1) and (J=3–2) emissions are close to thermalization and that the material dominating the emission is dense ($n_{H_2} \sim 10^4\, cm^{-3}$), cold ($T_k \leq 10K$) and distributed in structures much smaller than our best resolution ($\sim 1000AU$).

The link between both sets of conclusions might be that surfaces of isodissipation of kinetic energy in laboratory flows are fractal and have area-perimeter dimensions comparable to that measured for molecular clouds. It is remarkable in particular that there is no difference between the excitation conditions of the gas emitting in the line wings and in the line cores. The important issue of the formation, lifetime and resilience of such a structure is presently an open question.

References

Anselmet, F., Gagne, Y., and Hopfinger, E. J. 1984, *J. Fluid Mech.*, **140**, 63.

Bazell, D. and Désert, F. X. 1988, *Ap. J.*, **333**, 353.

Boissé P. 1990, *Astron. Astrophys.*, **228**, 483.

Boreiko, R.T., Betz, A.L., and Zmuidzinas, J. 1990, *Ap. J.*, **353**, 181.

Casoli, F., Dupraz, C., Combes, F., and Kazes, I. 1991 *Astr. Ap.* submitted.

Clemens, D.P., and Barvainis, R. 1988, *Ap. J. Supp.*, **68**, 257.

Drdla K., Knapp G.R. and van Dishoeck E.F. 1989, *Ap. J.*, **345**, 815.

Elmegreen, B.G. : 1991, these proceedings.

Falgarone, E., and Pérault, M. : 1987, *Physical Processes in Interstellar Clouds*, eds. G.E. Morfill and M. Scholer, Kluwer Acad. Publ..

Falgarone, E., and Pérault, M. : 1988, *Astr. Ap.*, **205**, L1.

Falgarone, E., and Phillips, T. G. 1990, *Ap. J.*, **359**, 344.

Falgarone E. 1991, *From Ground-based to Space-borne Submillimeter Astronomy*, eds. N. Longdon and B. Kaldeich, ESA Publ..

Falgarone, E., Phillips, T. G., and Walker C. 1991, submitted to *Ap. J.*.

Falgarone, E., Puget, J.-L., and Pérault, M. 1991, in preparation.

Frerking M.A., Keene J.B., Blake G.A., and Phillips T.G. 1989, *Ap. J.*, **344**, 311.

Frisch, U., Sulem, P. L., and Nelkin, M. 1978, *J. Fluid Mech.*, **87**, 719.

Genzel, R., Harris, A.I., Jaffe, D.T. and Stutzki J. 1988, *Ap. J.*, **332**, 1049.
Heithausen, A., and Thaddeus, P. 1990, *Ap. J. Letters*, **353**, L49.
Jaffe D.T., Genzel R., Harris A.I., Howe J.E., Stacey G.J., Stutzki J. 1990, *Ap. J.*, **353**, 193.
Keene, J., Blake, G.A., Phillips, T.G., Huggins, P.J., and Beichman, C.A. 1985, *Ap. J.*, **299**, 967.
Keto, E.R., and Lattanzio, J.C. 1989, *Ap. J.*, **346**, 184.
Kolmogorov A.N. 1941 : *Dokl. Akad. Nauk.* **26**, 115.
Kolmogorov, A. N. 1962, *J. Fluid Mech.*, **13**, 82.
Landau, L. D. and Lifchitz, E. M. 1959, *Fluid Mechanics*, Addison-Wesley.
Langer, W.D., and Penzias, A.A. 1990, *Ap. J.* in press.
Larson, R.B. : 1981, *Monthly Notices Roy. Astron. Soc.*, **194**, 809.
Lee, Y., Snell, R.L. and Dickman, R.L. 1990, *Ap. J.*, **355**, 536.
Lovejoy, S. 1982, *Science*, **216**, 185.
Magnani L., Blitz L., and Wendel A. 1988, *Ap. J.(Letters)*, **331**, L127.
Magnani L., Carpenter, J.M., Blitz L., Kassim, N.E. and Nath B.B. 1990, *Ap. J. Suppl.*, **73**, 747.
Mandelbrot, B. B. 1982, *The fractal geometry of nature*, Freeman.
Mauersberger R., Henkel C., Wilson T.L. and Harju J. 1990, *Astron. Astrophys.*, **223**, 79.
Méneveau 1989, PhD. dissertation, Yale University.
Mooney, T.J., and Solomon, P.M. 1990 in preparation.
Oboukhov, A.M. 1962, *J. Fluid Mech.*, **13**, 77.
Penzias, A.A., Solomon, P.M., Jefferts, K.B., and Wilson, R.W. 1972, *Ap. J. Letters*, **174**, L43.
Pérault M., Falgarone E., and Puget J.L. 1985, *Astr. Ap.*, **152**, 371.
Phillips, T.G., and Huggins, P.J. 1981, *Ap. J.*, **251**, 533.
Sage L.J., Shore S.N. and Solomon P.M. 1990, *Ap. J.*, **351**, 422.
Scalo, J. : 1987, *Interstellar Processes*, eds. D.J. Hollenbach and H.A. Thronson.
Scalo, J.M. 1990 *Physical Processes in Fragmentation and Star Formation*, eds R. Capuzzo-Dolcetta et al., Kluwer Academic Publ. : Dordrecht.
Sreenivasan, K. R. and Méneveau, C. 1986, *J. Fluid Mech.*, **173**, 357.
Stutzki J., Stacey, G.J., Genzel, R., Harris, A.I., Jaffe, D.T., and Lugten, J.B. 1988, *Ap. J.*, **332**, 379.
Ungerechts, H. and Thaddeus, P. 1987, *Ap. J. Suppl.*, **63**, 645.
van Atta, C. W. and Park, J. 1971, *Statistical Models and Turbulence*, eds. M. Rosenblatt and C. van Atta : Springer.
Wakker, B.P., 1990, Ph.D. Dissertation, University of Leiden.
Zmuidzinas, J., Betz, A.L., Boreiko, R.T., Goldhaber, D.M. 1988, *Ap. J.*, **335**, 774.
Zuckerman, B. and Evans, N.J. 1974, *Ap. J.*, **192**, L149.